



NATIONAL INSTITUTE OF TECHNOLOGY

TIRUCHIRAPPALLI

Summer Internship Report

CMS-GEM LAB, CERN, GENEVA

Gas Electron Multiplier Detectors

Author:

Pratik JAWAHAR

Supervisors:

Dr. Michele BIANCO

Dr. Jeremie MERLIN

July 23 2018

Abstract

Gas Electron Multipliers (GEM) are an advanced group of detectors, capable of detecting sub-atomic particles such as muons and generating an estimate of the particle trajectory. Muons are one of the myriad of particles produced by proton-proton collisions in the Large Hadron Collider (LHC). The LHC is the main particle accelerator at CERN, the European Center for Nuclear Research and GEM Detectors are being used in major experiments at various points of the LHC, such as Atlas and CMS. The GEM Detectors have been viewed as the next step in Particle Detector Technology after the Resistive Plate Chamber (RPC) and the Cathode Strip Chamber (CSC). The GEM Detectors were first conceptualized by Fabio Sauli at CERN in 1997, and have developed to become one of the most sophisticated and accurate particle detector systems of current times. However, they have not completely replaced the RPC or CSC yet, but provide crucial redundancy and will be utilized more integrally once the High Luminosity upgrade on the LHC is complete (HL-LHC). The CMS GEM Collaboration has decided to currently utilize and test the GEM Detectors, called GE1/1 Chambers, in the muon end-caps.

This report gives a detailed account of the various activities undertaken during the summer internship at the CMS-GEM Lab. Tasks such as assembly of the GEM Super-chambers, Quality Control Tests on assembled chambers, design and setting up of testing rigs to monitor certain parameters of the detectors such as planarity, and design of few other minor mechanical components were undertaken and are thereby presented in this report with commensurate results.

Contents

1 The GEM Technology	3
1.1 The Single GEM Detector	3
1.1.1 Influence of Electric Field	6
1.1.2 Influence of Gap Thickness	7
1.1.3 The GEM Voltage	8
1.2 The Triple GEM Detector	9
1.2.1 Transfer Electric Field	9
1.2.2 Transfer Gap Thickness	10
1.2.3 The GEM Voltages	12
1.3 Parameters that affect performance of GEM Foils	13
1.3.1 Influence of hole diameter on performance	13
1.3.2 Influence of hole pitch	13
1.3.3 Influence of hole shape	14
2 The GE1/1 Chamber	15
2.1 General Design	15
2.2 The Drift Board	16
2.3 External Frame Design	18
2.4 Internal Frame Design	18
2.5 The GEM Foil	20
2.6 Gas Distribution System	21
2.7 The Readout Board	21
2.8 Readout Electronics	22
3 GE1/1 Detector Assembly	23
3.1 Drift Board Preparation	23
3.2 GEM Stack Assembly	24
3.3 Chamber Construction	25
3.4 Stretching Mechanism	25
4 Chamber Assembly and QC Tests Performed	26
4.1 Chamber GE1/1-X-L-CERN-0037	26
4.1.1 Particulate Matter Burn Out	27
4.2 Chamber GE1/1-X-L-CERN-0038	27

1 The GEM Technology

The GEM technology is heavily dependent on the GEM foil which is a thin Kapton foil, coated with a very thin layer of copper on both sides. The thickness of the Kapton foil and copper coating are $50\mu\text{m}$ and $5\mu\text{m}$ respectively. The foil has numerous, specially etched holes that aid in the electron multiplication process. Each hole has an external diameter of $70\mu\text{m}$, an internal diameter of $50\mu\text{m}$ and a pitch of $140\mu\text{m}$. An ionization in the gas mixture by radiation releases electrons which drift into the holes, where there is a strong electric field ($\sim 100\text{kV/cm}$), for an applied potential difference of $300 - 500\text{V}$ between the two copper sides of the foil. This region inside the hole is suitable for accelerating the electron such that it acquires enough energy to create an avalanche. The gain that can be achieved with a single GEM foil is over 10^3 .



Figure 1: Insert image here

The holes are produced using the conventional photolithographic technique, where the material to be etched is coated with a photoresist and selectively etched using UV radiation by employing a masking technique. The challenge however lies in aligning the masks on the top and bottom surfaces of the foil perfectly, else one side of the foil may be over-etched leaving the other side under-etched and this will affect all performance parameters drastically. Shown below is a diagram of the production process.

1.1 The Single GEM Detector

The simplest GEM detector is the single GEM, which consists of one GEM foil sandwiched between two electrodes, the drift board (cathode) and the



Figure 2: Insert image here

readout board (anode). The electric field E_d in the Drift Gap is generated due to the potential difference between the top of the foil and the drift board, while the field E_i in the Induction Gap is generated due to the potential difference between the bottom of the foil and the readout board.



Figure 3: Insert image here

When a charged particle crosses the detector, it produces primary ions and electrons in the drift gap. These ionization electrons follow the drift field lines into the hole. The electric field density inside the hole is significantly higher which results in acceleration of the electron, thereby increasing the number of collisions within the hole. This cause more ionization and this process of electron multiplication is called electron cloud density amplification. Some of the multiplication electrons are collected at the lower part of

the foil, while most of the multiplication electrons pass into the Induction Gap. Typically the fraction of electrons that pass into the induction region is $\sim 50\%$. This value depends on the strength of the electric field inside the hole and on E_i . The multiplication electrons that pass into the induction gap are responsible for producing an induced current on the readout board (anode).



Figure 4: Insert image here

The readout board is generally a simple PCB whose structure is defined based on the need. They are produced using strips or pads of connectors whose shape can be chosen as required, and are connected to the front-end electronics. The readout is kept at ground potential which also consequently helps in the simplification of front-end electronics.



Figure 5: Insert image here

Thus, the induced signal is purely due to the movement of the electrons in the induction gap. The major parameters that affect the performance of the single GEM detector are,

- Electric Field in Drift and Induction Gaps
- Thickness of the Drift and Induction region
- Voltage Difference applied to the GEM foil

1.1.1 Influence of Electric Field

The field lines in the drift and induction gaps are similar to a parallel plate capacitor, with increasing field line density near the holes.

The Drift Field

The purpose of the drift field, as the name suggests is to collect and draw the primary electrons, produced by the ionization, into the GEM holes. Shown below is a comparison of the relative signal amplitude as a function of the drift field, deduced from a measurement of current and from pulse height with two shaping times (100ns and 1 μ s).



Figure 6: Insert image here

At low field values ($< 0.5kV/cm$), the curves drop due to a low electron drift velocity and large diffusion. At intermediate value ($\sim 1/3kV/cm$), the signals reaches a plateau and decrease again for higher value of drift field. In $Ar/CO_2(70/30)$ gas mixture the typical value of the drift field is $2kV/cm$.

The Induction Field

The purpose of the induction field is to extract the multiplied electrons from the GEM holes and to transfer them towards the readout board (anode). At very low values of the induction field all the secondary electrons, extracted from the GEM holes, are practically collected on the bottom of the GEM foil and the induced signal becomes weaker (Ramo-theorem). Increasing the induction field value causes a larger part of the secondary electrons to be collected on the readout electrode thereby increasing the induced current on the readout board and decreasing the induced current on the bottom of the GEM foil. At higher induction field values, $E_I > 8\text{kV/cm}$, discharges on the anode can occur due to the high electric field in proximity to the edges of the readout electrode. Irrespective of the gas mixture used, a value of the induction field of $\sim 5\text{kV/cm}$ is a reasonable compromise and allows to collect a large fraction (50%) of the charge on PCB.

1.1.2 Influence of Gap Thickness

The Drift Gap

The geometry of the drift gap was chosen to ensure a high particle detection efficiency. For a charged track, the number of electrons clusters created has a Poisson distribution with an average value \bar{n} depending on the particle energy and the gas mixture used. For any reasonable choice of the gas mixture, a 3mm wide gap guarantees the full efficiency of the detector. A wider drift gap should essentially leave the detector efficiency unchanged, while it can increase the pile-up effects at very high particle rate as well as the aging rate. In fact, the charge integrated by the detector obviously linearly depends on the value of the primary electrons released in the drift gap.

The Induction Gap

The induction gap is typically 1 mm thick in order to maximize the signal fraction integrated by the amplifier. The GEM signal amplitude is proportional to the ratio between the electron drift velocity and the thickness of the induction gap. This consideration suggests both the use of a fast gas mixture and a small thickness for the induction gap. However, a gap width less than the order of a millimeter is not advised because it would require a high mechanical tolerance in order to avoid discharges on the PCB, and obtain non uniformity of detector.

1.1.3 The GEM Voltage

The voltage V_{GEM} applied to the GEM foil is responsible for the generation of electric field in the holes. The intrinsic gain also depends directly on the V_{GEM} value, as seen below.

$$G_{intrinsic} \propto e^{<\alpha>V_{GEM}}$$

where, $<\alpha>$ is the average of the first Townsend coefficient along the electron path through the hole. This coefficient is dependent on the gas mixture and the electric field. The intrinsic gain can reach values of the order of 10^3 . However, due to dispersive effects, the effective number of electrons transferred to the anode decreases and thus the effective gain is less than the intrinsic gain.

Important parameters to study the GEM chambers are:

1. Collection efficiency (ϵ^{coll}) :

$$\epsilon^{coll} = \frac{\text{No.of electrons collected in the holes}}{\text{No.of electrons produced above the holes}}$$

represents the ratio between the number of electrons entering the multiplication channels and the number of primary electrons generated above the GEM. The collection efficiency is generally a function of the electric field above the GEM and the electric field inside the hole.

2. Extraction fraction (f^{extr}) :

$$f^{extr} = \frac{\text{No.of electrons extracted from the holes}}{\text{No.of electrons produced in the holes}}$$

represents the ratio between the number of electrons extracted from the holes and transferred to the PCB and the number of electrons multiplied inside the amplification channels. The extraction fraction is a function of the electric field inside the hole and the electric field below the GEM.

1.2 The Triple GEM Detector

The Triple GEM detector is similar to the single GEM except for the fact that three GEM foils are stacked and sandwiched between the Drift board and the Readout board instead of just one foil. The use of three foils instead of one implies higher effective gain values can be attained without the need for providing a very high potential difference.



Figure 7: Insert image here

The discussion on the working of the single GEM chamber allows for easier understanding of the working of the triple GEM chamber. The internal structure of the triple GEM is shown below with the respective gap widths. The gap between the Drift board and the top of the first GEM foil is called the Drift gap and that between the Readout board and the bottom of the third GEM foil is called the induction gap. The gaps between the foils are labeled transfer gap 1 and 2 respectively.

The same considerations apply to both the single and triple GEM chambers in case of electric fields and geometric thickness of the gaps. However, the transfer region acts as a drift gap with respect to the GEM below and as an induction gap with respect to the GEM above. Thus, special considerations for electric fields and thickness of the transfer gaps are essential.

1.2.1 Transfer Electric Field

The major purpose of the transfer electric field is to transport the secondary electrons produced in the GEM hole above, into the GEM hole below. The value of this electric field is to be selected keeping in mind the fact that as a



Figure 8: Insert image here

result, the extraction fraction of the upper GEM foil and collection efficiency of the lower GEM foil are both maximized simultaneously. It is observed that at low transfer field values ($E_T < 3\text{kV/cm}$) the extraction fraction is so low that the multiplication electrons are extracted by the upper GEM holes but are mainly collected on the bottom electrode of the foil. On the other hand at higher field values ($E_T > 4\text{kV/cm}$) the collection efficiency decreases owing to a high defocussing effect.

1.2.2 Transfer Gap Thickness

In order to improve the time performance of the detector and to keep the discharge probability to a minimum, several tests were performed using different sizes of the transfer gaps, using the following detector geometry ($g_D/g_{T1}/g_{T2}/g_I$) : 3/2/2/1, 3/1/2/1 and 3/1/1/1.

First Transfer Gap

When a charged particle crosses the detector it causes the gas to ionize in each of the gaps. The main difference is that the electrons produced in the drift gap undergo multiplication through all three multiplication steps while those produced in the other gaps go through two or less multiplications stages. However, the ionization produced in the first transfer gap and multiplied by the next two GEM foils produces a signal on the readout board large enough to be detected by the front-end electronics. This signal, depends on the drift velocity of the gas mixture and the gap thickness, and it is calculated, with respect to the signal produced by a primary electron coming from the drift

gap, bears the relation, $\Delta t = g_t/v_{drift}$. This effect, particularly important for the time performance of the detector, is called bi-GEM effect. For an electric field of $3kV/cm$, the electron drift velocity of this gas mixture is about $100\mu m/ns$. With a $2mm$ gap, the time spectrum is characterized by the presence of small amplitude events in advance of $\sim 20ns$ with respect to the main signal, broadening the distribution. A 5% of the total number of events are represented by bi-GEM events. Vice versa with a $1mm$ thickness the anticipated signals, in this case in advance of $\sim 10ns$ with respect to the main signal, are practically disappeared, being reabsorbed by the global fluctuations of the arrival time of the electrons. In this case, the bi-GEM events are less than 2% of the total. This result suggests that the thickness of the first transfer gap has to be keep as low as possible. The value of g_{T1} is set to $1mm$.

Second Transfer Gap

The primary electrons produced in this gap undergo multiplication only through the last GEM foil. Hence, it is highly improbable for these primary electrons to undergo multiplication enough to generate a signal above the threshold value at the readout board. The thickness of this gap is thus mainly correlated with the discharge probability which is basically the probability of having a discharge within the GEM hole when the number of electron-ion pairs exceeds the Raether limit in the third multiplication stage.



Figure 9: Insert image here

The most common method to reduce discharge probability is to mix a quencher gas in the gas mixture. The ageing characteristics of the detector decide the type and quantity of quenching gas to be used for optimal

performance, longevity of the detector and low discharge probability. For a triple-GEM chamber however, increasing the width of the second transfer gap helps reduce the discharge probability. When the thickness of the gap is increased, it allows for more diffusion of the electron cloud, which spreads out laterally proportional to the square root of the drift velocity. This means the electron cloud spreads over a larger area than just one GEM hole. This prevents the number of electron-ion pairs exceeding the Raether limit in each hole, thereby decreasing the discharge probability. Taking these factors into consideration with a sufficient factor of safety, a gap thickness of $2mm$ was decided upon.

1.2.3 The GEM Voltages

The intrinsic gain of a triple-GEM chamber is an exponential function of V_{GEM}^{tot} . Incorporating the electric fields of the various gaps and the total electron transparency (T_{tot}) the effective gain of the detector is given by:

$$G_{eff} = G_{intr}.T_{tot} = \prod_{k=1}^3 e^{<\alpha>_k \cdot V_{GEMk}} \cdot T_k = e^{<\alpha>^{tot} \cdot V_{GEM}^{tot}} \cdot \prod_{k=1}^3 \epsilon_k^{coll} \cdot f_k^{extr}$$

where the $<\alpha>$ is the average of the first Townsend coefficient of the electron path through the hole, ϵ_k^{coll} and f_k^{extr} are the collection efficiency and the extraction fraction of the k^{th} GEM foil respectively. The effective gain only depends on the net voltage applied to the three GEM foils so its possible to alter the voltage difference across each foil in a manner that decreases the discharge probability at the last GEM foil. For a fixed gain, it is convenient to increase the voltage applied on the first GEM foil while reducing it to the third GEM foil. In this case, the charge accumulated on the third GEM is greater but the diffusion effect allows the electron cloud to be spread over a larger number of holes, thereby reducing the discharge probability. The optimal configuration is found to be:

$$V_{GEM1} \gg V_{GEM2} \geq V_{GEM3}$$

This GEM voltage configuration reduces the discharge effect and also improves the detector time performance. Simultaneously, the collection efficiency on the first GEM can increase slightly due to a reduction of the defocusing effect.

1.3 Parameters that affect performance of GEM Foils

1.3.1 Influence of hole diameter on performance

The diameter of the hole is an important factor that controls the energy acquired by the electron passing through it. Since the electric flux inside the hole can be increased by either increasing the potential difference between the two ends of the foil or by decreasing the area of the hole, the diameter of the hole indirectly controls the acceleration and thereby the energy acquired by the electron which eventually decides if the gain produced is sufficient enough. Shown below is the correlation between the effective gain and the hole diameter, for the same gas mixture at the same electric field.



Figure 10: Insert image here

A saturation effect is observed below $70\mu\text{m}$, which is due to the increasing probability for electrons from the avalanche to diffuse into the lower electrode at lower diameters as the avalanche is forced to flow close to the lower electrode when the diameter is low. This however has the positive effect that gain is not heavily dependent on the precision of the manufacturing process beyond a certain extent.

1.3.2 Influence of hole pitch

The hole pitch does not affect the gain value directly, but affects a parameter known as collection efficiency of electrons in the GEM hole. The collection efficiency is dependent on many factors and effects but mainly describes the measure of the electron losses while crossing the hole. This is dependent on

the electron transparency of the foil which is the ratio between the total area of the holes and the total area of the foil. Electron transparency is similar in sense to optical transparency, the equation for which is $t = D^2/2\sqrt{3}P^2$, where D is the diameter and P is the pitch of the hole. Evidently, lower pitch value results in higher electron transparency and this results in higher collection efficiency.



Figure 11: Insert image here

1.3.3 Influence of hole shape

The hole shape is mainly responsible for a short term charging-up effect that alters the gain slightly. This is rate-dependent and can be minimized by altering the shape of the hole. The main cause of this effect is the Kapton insulation present very close to the multiplication channels. The electrons and ions from the avalanche accumulate on the kapton surface as a result of which the electric field in the multiplication channels is altered. The geometry that best minimizes this effect was found to be a cylindrical shape as seen below. However the bi-conical shape was chosen considering ease of production as compared to the conical shape, with a minor compromise on the charging-up effect.



Figure 12: Insert image here

2 The GE1/1 Chamber

2.1 General Design

The GE1/1 chamber is a triple-GEM detector. The gross external frame of the detector is trapezoidal, and the detector itself is made of a drift board, a stack of three identical GEM foils, the readout board and the external gas frame as shown in Fig.14. The gap between the drift board and the first GEM foil is called the drift gap and the subsequent gaps are called the transfer-1, transfer-2 and the induction field gap respectively. The widths of the drift gap, transfer-1, transfer-2 and induction field gap are 3mm, 1mm, 2mm and 1mm respectively. The GE1/1 chambers are assembled in two types namely the Long and the Short, which differ only in length.

The design of each component is dealt with individually in the following sections.

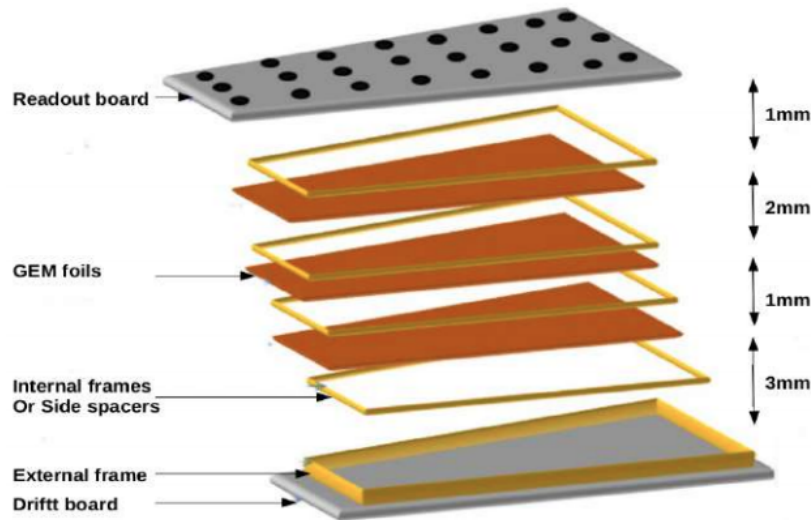


Figure 13: GE1/1 Prototype

2.2 The Drift Board

The Drift Board lies on the bottom of the chamber as shown in Fig.14. It is a Printed Circuit Board (PCB) that holds the trapezoidal drift electrode. The active area of the board is coated with a copper layer, which is in contact with the gas mixture in the detector. The figure below shows the CAD drawing for the Drift Board.

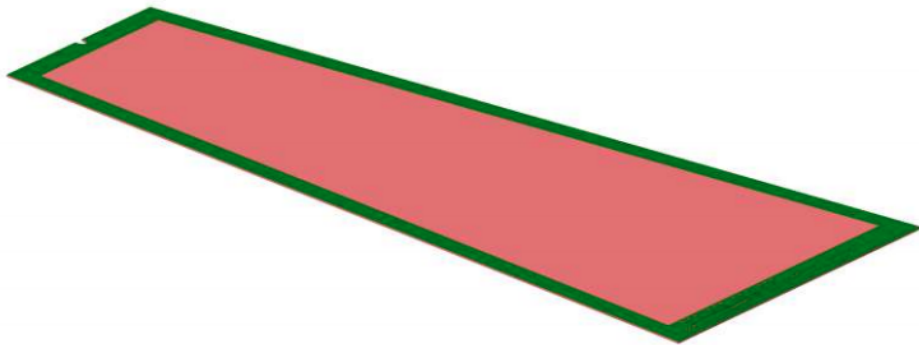


Figure 14: Drift Board Mechanical Draw

The board also houses the spring loaded High Voltage (HV) pins which

are used to power the GEM foils. Four pins are used to power each foil, two for the top of each foil and two for the bottom. The positions of the pins are defined corresponding to the HV pads on each foil. The HV pins corresponding to one foil are of the same height but vary in height from the pins of another foil. The height of the pins is calculated according to the height of the corresponding GEM foil from the drift board. Consequently there are 12 pins on the drift board positioned relevantly.

On the periphery of the board there are multiple through-holes to mount the stainless steel Pull-Outs on the board. These Pull-Outs are important parts of the mechanism that stretches the GEM foils. The need for stretching is explained in Sec. Refer the stretching section. Fig.15 shows the view of the HV connections on the drift board up close.

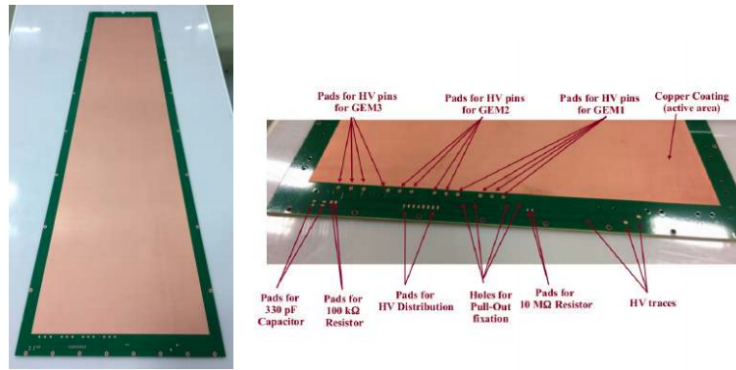


Figure 15: a) Image of the Drift Board(left) b) Zoomed image of the HV connections on the Drift Board(right)

The other elements on the board as shown in Fig.15 are the HV traces, a dedicated pad for a $10M\Omega$ resistor and pads for a decoupling RC circuit.

The $10M\Omega$ resistor ensures the safety of the detector from electrical damage that might arise as a result of the high voltage of operation. The decoupling RC circuit consists of a $100k\Omega$ resistor and a $330pF$ capacitor. This is used to decouple the trigger signal from the HV signal when the readings are acquired from the bottom of the GEM-3 foil.

2.3 External Frame Design

The external frame is a trapezoidal structure as shown in Fig.16 made of halogen-free glass-epoxy material and is machined from a single piece to minimize material non-homogeneity. The frame is primarily used to make the chamber gas tight, by closing in the active gas volume between the drift and readout boards.

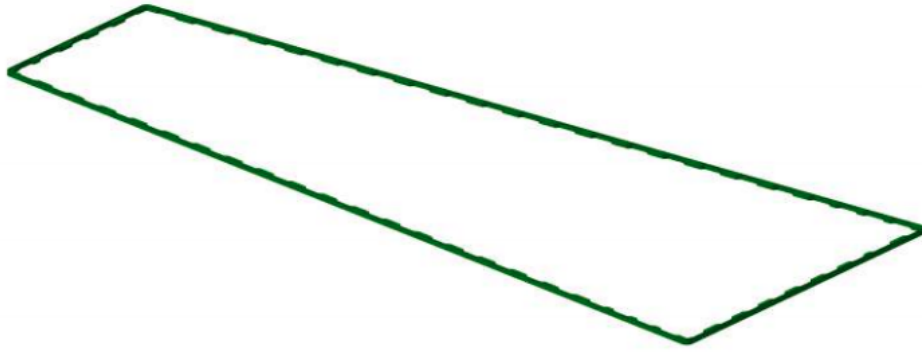


Figure 16: Model of the External Frame

The external frame also has a small groove along its periphery to accommodate the Viton O-ring that compresses between the drift and readout boards, thereby ensuring a greater degree of gas-tightness without damage or deformation to the frame or any other components. The frame also has notches all around to accommodate the Pull-Outs as shown in Fig.17

A Nuvovern polyurethane varnish coating is applied on the frame to seal in the particulates such that it does not contaminate the detector with particulate matter during assembly.

2.4 Internal Frame Design

The internal frames are important components as they ensure the proper spacing between each of the gaps in the stack. There are four layers of internal frames, made of halogen-free epoxy glass as shown in Fig.18.

The frames are coated with a Nuvovern polyurethane varnish coating, to compact the particulate matter such that it does not contaminate the clean room or the detector with dust. Dust on the GEM foils is most often

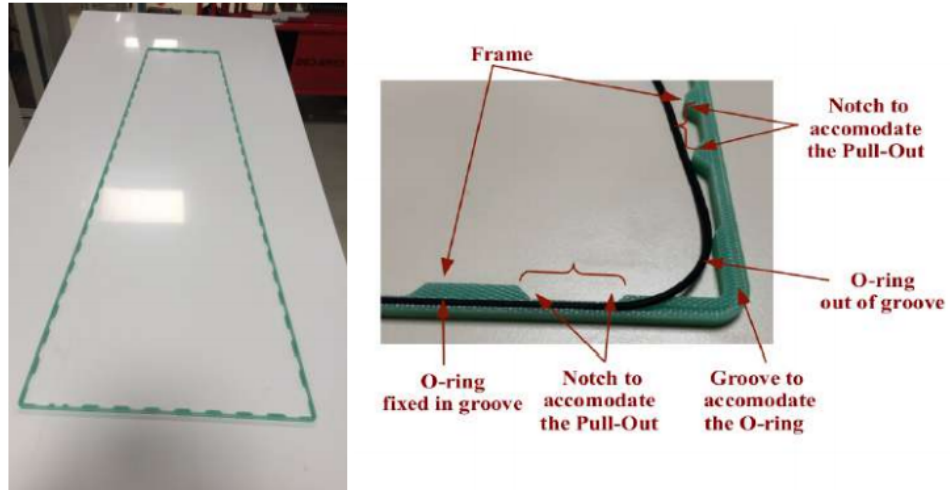


Figure 17: a) Image of the External Frame(left) b) Zoomed image of one segment of the External Frame(right)

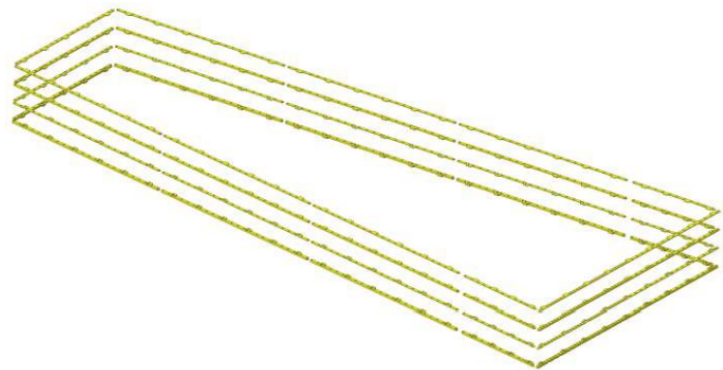


Figure 18: Drawing of the Internal Frame Stack

responsible for the production of electrical shorts and sparks in the holes and thus potentially causing damage to the foil. Hence the varnish coating also helps avoid this problem.

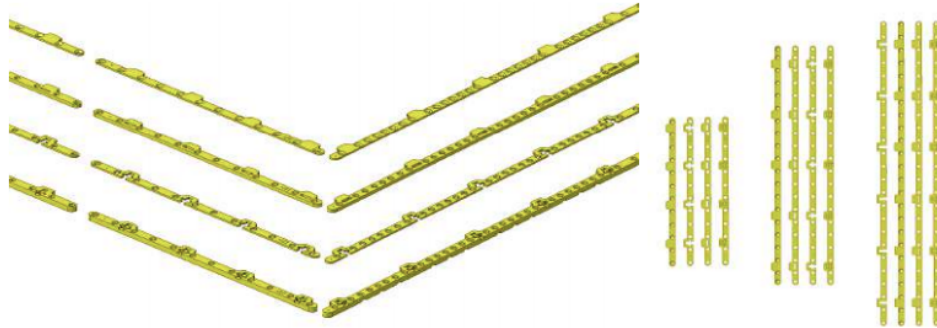


Figure 19: a) Drawing of one Internal Frame sector(left) b) Mechanical structure of the different Internal Frames(right)

The thickness of each layer is 3mm, 1mm, 2mm and 1mm respectively and each layer is made of ten individual pieces.

Threaded *M2* brass inserts are fitted in the 3mm frame to avoid loosening of macroscopic and microscopic epoxy glass particulates that may arise when screws pass through the frames during assembly.

2.5 The GEM Foil

The GE1/1 chamber is a triple GEM detector. It hence consists of three identical, trapezoidal GEM foils as shown in Fig.20. The GEM foils are produced at the CERN PCB workshop using a the single mask production technique which is a type of chemical etching.

The surface of the foil oriented towards the Readout Boards is a single continuous conductor whereas the other surface, oriented towards the Drift Board is segmented into strips. These strips are aligned parallel to the base of the trapezoid and the width of each strip reduces as we move from the short edge to the long edge of the trapezoid. This is to ensure that the area of each strip is the same and approximately equal to 100cm^2 . The amount of charge that can possibly generate during a discharge is constrained by the

segmentation in the foil, thereby limiting the total energy of a discharge. Another advantage of segmentation is that even in extreme cases such as destructive discharge causing a short in one particular HV sector, only that sector is rendered useless and not the entire foil. This however bears the implication that each sector has to have a separate HV supply. This is dealt with by choosing a common connection point that receives the external HV supply and routing a HV trace from it along the periphery of the GEM foil. The common connection points are placed on the wide end of the foil and two connection points are added for redundancy. The HV trace is connected to the foils through $10M\Omega$ protection resistors that are mounted on the surface. These resistors limit the current supplied from HV supply, decouple the capacitance from all other HV sectors and to quench the discharge.

2.6 Gas Distribution System

The gas distribution system on the GE1/1 chambers is a single inlet, single outlet system. As mentioned in the previous section the inlet and outlet gas plugs are mounted at diagonally opposite points on the readout board. One such gas plug is showed in Fig..

The gas mixture is flows into the chamber through the inlet diagonally. The thin and stretched GEM foils direct the flow to the other corners of the detector and since the foils are stretched they make the flow almost laminar. The gas distribution within the GEM foil stack occurs by means of the holes in the foil and through the gaps in the internal frames.

2.7 The Readout Board

The readout board is a PCB that lies just above GEM-3 as shown in Fig.14. It has a trapezoidal shape and it contains 3072 radial readout strips on its inner side.

The area covered by the strips is called the active area and it subtends an angle of 10.15° . This allows for an over lap of $2.6mrad$ (5.67 strips) between the active area of subsequent chambers. The readout strips are connected through metalized vias to the other side of the board, from which traces are routed to 8×3 partitions in $(i\eta, i\phi)$. Each $(i\eta, i\phi)$ sector contains 128 strips. The strip pitch increases from $0.6mm$ at the shorter end of the detector to $1.2mm$ at the wider end. The readout board also has two diagonally opposite

holes on the corners to accommodate the gas plugs that will serve as the inlet and outlet respectively, as explained in Sec.2.6.

2.8 Readout Electronics

As mentioned in the previous section, the *GE1/1* chamber consists of 128 channels per sector leading to a total of 3072 readout strips per chamber distributed over 8 η -partitions. Each 128 channel connector is connected to the VFAT3 front-end ASIC. The VFAT3 is an electronic chip that consists of 128 channels and each consists of a charge sensitive pre-amplifier, a shaper and a constant fraction discriminator. The data signals from each channels is synchronized with the $40MHz$ LHC clock. It is split into two, one with a fixed latency for the trigger signal and a second signal with variable latency for tracking data. A multi-layer PCB called the GEM Electronics Board (GEB) is placed on the readout board and E-Links are used to power, control and obtain the readout signals from the VFAT3. The Opto-Hybrid (OH) board acts as the interface between the front-end electronics and the off-detector systems. The OH helps accommodate a unidirectional optical path, to transfer the fixed latency trigger from the VFAT3 to the CSC system, and a bidirectional path that connects the OH to the back-end electronics. The bidirectional path is also responsible for carrying the tracking and triggering data from the ASIC. It also carries the configuration and control commands such as power supply, threshold and readout settings. The back-end electronics is based on the μ TCA standard, recently developed for the telecommunication industry and adopted by CMS to replace the VME electronics. This provides a compact design capable of very high data throughput (2Tbits/s) with high availability. For the GEM chamber, μ TCA crates are equipped with eight Advanced Mezzanine Cards (AMC) based on the Virtex 7 FPGA (MP7). The first Carrier Hub (MCH) slot is occupied by a commercial MCH that provides a Gigabit Ethernet (GbE) communication for the Slow controls and the configuration signals. The second slot is reserved for a CMS standard MCH module called AMC13 to interface the crate to the CMS DAQ system and take care of the Trigger, Timing and Control (TTC) signals.

3 GE1/1 Detector Assembly

The GEM technology heavily depends on the integrity of the GEM foils and its precision-etched micron level holes. Even the smallest of particulate contaminant can become a source for irregular operation or may even cause unreparable damage to the detector. Thus, assembly can only be performed within a clean room with a class-1000 rating at the very least. Fig.23 shows an overview of the critical steps to be performed during assembly and is a representation of the overall flow of the assembly procedure.

People performing the assembly strictly abide by the code of conduct within the clean room such as wearing aprons, dust-free gloves, facial masks, shoe covers, hair caps etc.

3.1 Drift Board Preparation

The drift board preparation includes the mounting of the stainless steel pull-outs and the soldering of 12 HV pins to power each layer. Since this involves soldering and manual fastening of screws, there is high scope for contamination and thereby this step is carried out outside the clean room. The heights of each set of HV pins are in accordance with the position of the respective GEM foils and are mounted on the drift board in that specific order. Each pull-out is fastened to the drift board using two A2 stainless steel $M3 \times 6 \times 8$ screws with poly-amide washers to ensure gas tight fastening. The surface mounted (SMD) $10M\Omega$ protection resistance and the decoupling RC circuit consisting of the $10k\Omega$ resistor and the $330pF$ capacitor are mounted in their respective positions at this stage.

The HV pins are designed to provide optimal and stable power supply to each foil. Their spring-loaded design allows for continuous contact with the corresponding pads of the GEM foil when the foil is mounted on the stack. The HV circuit design on the drift board is shown in Fig.24.

The pads on the foils are designed to be used with both single channel and multi channel power supply. In case of a single channel power supply a resistive HV divider network is used to supply appropriate voltage distribution within the chamber.

Figs.25, 26 and 27 show the design and arrangement of the HV pins on the drift board and their positions with respect to the GEM foil stack.

3.2 GEM Stack Assembly

The most important part of the assembly is preparing the GEM Stack which is a precarious process as it deals with the careful alignment of the parts without any scope for contamination. This step is performed within the clean room. The alignment is done using alignment pins on a Plexiglas base. The alignment pins are placed at precise positions in correspondence to the alignment holes on the FR4 pieces that hold each GEM foil. The 10 pieces of the $3mm$ internal frame are first placed in proper positions before the first GEM foil is placed as shown in Fig.28.

The GEM foil has to be cleaned again as a precautionary measure just before aligning them on top of the first external frame layer. This is carried out using an anti-static adhesive roller which can remove dust with micron level precision as shown in Fig.29a).

The next step in the assembly is the test for measuring the leakage current using the MEGGER MIT420. In this step a $550V$ potential difference is applied across the foils which produces a strong electric field, generally of the order of $70-100keV$ inside the GEM holes. When the relative humidity (RH) of the area is 30% or less, the maximum permissible leakage current is $35nA$ for an applied potential difference of $550V$. Above 30% the leakage current increases drastically. Minor sparks may be observed during this procedure. This is caused small particulate matter trapped between the holes. The spark burns out the small particles and thus serves as a secondary cleaning procedure. Excessive rate of sparking however implies that the GEM foils are contaminated with dust and the primary foil cleaning procedures are to be repeated. As a result of this test, the holes accumulate electrostatic charges and by virtue of this might start catching dust themselves. Also, if the GEM foils on the stack happen to come in contact with each other prior to the stretching procedure, the accumulated energy might get released at the point-like contact, thereby leading to destructive discharges that might ruin the integrity of either or both of the foils. For these reasons, the foils must be discharged after the leakage current test by shorting the top and bottom electrodes of the foil.

As a precautionary measure, the gem foils are stretched manually and fixed temporarily using tape between the stretched outer holding frame of the foil (which is cut out in a later step) and the Plexiglas base. This prevents the foils from sagging and coming in contact with each other during the aligning of the foils in the stack, prior to the implementation of the stretching

procedure.

The foils are aligned in the stack using the alignment holes as seen in Fig.20 and are attached to the internal frames using the pattern of holes meant to align the fasteners. The foil stack is held in place by multiple $M2 \times 6$ screws, that run through all the internal frame segments and are tightened against the $M2$ brass inserts shown in Fig.30. The stretching nuts are positioned in dedicated plus-shaped grooves at this point in the assembly, with their axes oriented perpendicular to the axes of the brass inserts in the internal frame.

The dead area around the foils is then cut out and the foil stack is ready for the next step. The various steps explained above are shown in Fig.31.

3.3 Chamber Construction

The chamber construction starts with the placement of the GEM stack on the drift board. The drift board is fixed in place by Aluminium bars. The jig keeps the drift board flat and prevents any kind of deformations that may occur during chamber construction. The stack is stretched against the pull-outs manually by applying a monitored torque. The stretching mechanism is dealt with in detail in the next section. Next, a connectivity check is performed between each of the gaps. This is performed using a Mega Ohm Insulation tester. The HV traces are used to apply a potential difference of 550V and the impedance is measured. At RH 30% an impedance of $100 - 150G\Omega$ is expected. At higher humidities, the impedance values are expected to decrease.

The external frame with the O-ring is placed and the readout board is placed over the external frame. The readout board is tightened against the pull-outs using A2 stainless steel $M3 \times 6 \times 8$ screws sealed with poly-amide washers. This causes the O-ring to deform and fill up the gaps forming a gas tight seal. The final chamber is showed in Fig..

3.4 Stretching Mechanism

After testing multiple stretching mechanisms like use of infrared heating lamps, fiberglass spacer frames etc. the mechanical stretching method was chosen owing to significant reduction in time consumed for stretching as compared to the other methods considered. Since no glue is used, the assembly time is reduced from a time dynamic of days to a few hours.

Once the stack is placed on the drift board, $M2.5 \times 8 \times 8$ screws are inserted around the periphery of the stack and are tightened manually into the perpendicular nuts that were previously placed into the grooves of the internal frame. These screws are manually tightened using a controlled and monitored torque of $8 - 10\text{cN} - \text{m}$. Thus the GEM foils are tensioned uniformly as they are stretched outwards all around the periphery as shown in Fig.36.

The torque specifications are to be followed with as much precision as possible since the inherent tolerances of this method have an effect on the uniformity of the gas gain and the time response. Thus abiding by the torque specifications carefully minimizes the non-uniformity in detector parameters and thereby the output parameters are uniform to the desired precision.

4 Chamber Assembly and QC Tests Performed

The naming of a detector gives all important details required to track the detector's performance right from assembly to installation. The GEM chamber nomenclature consists of 5 parts namely: chamber type, generation number, external dimensions (L- long; S- short), name of production site and finally the detector number in order. An example for this is GE1/1-VIII-S-CERN-0001, where GE1/1 is the type which defines at which position of Point 5 on the LHC the detector chamber will be mounted, VIII stands for 8th Generation, S stands for short type, CERN is where the detector was produced and 0001 is the chamber batch number.

4.1 Chamber GE1/1-X-L-CERN-0037

The GE1/1-X-L-CERN-0037 or chamber number 37 as the name suggests is a tenth generation chamber, which signifies that it is the final version that will be installed at Point 5 on the CMS end caps during the *LS1*. This chamber displayed some very anomalous behavior right from the assembly stage.

During the QC2 test while assembling, the GEM foils underwent a lot of sparking which might have been a result of particulate matter trapped in the holes. A secondary cleaning procedure was performed and after multiple tests with the MEGGER the chamber was finally cleared through QC2.

During the gas leak test or the QC3, the chamber performed well on the first trial with a gas leak of 4.8mBar/h which is below the safe limit and hence the chamber passed the Gas Leak test. After a 15h flushing period, the standard QC4 procedure was initiated to perform the High Voltage Test. The chamber produced good results initially during the slow ramp up period up to 4.3kV of input supply. However, beyond 4.3kV the chamber started behaving strangely and the rate of the spurious signal suddenly spiked from 346 counts per minute to over a million counts in one minute. Standard trouble shooting procedures were followed to try identify the causes of the problem.

4.1.1 Particulate Matter Burn Out

The suspected reason for the sudden spike in the rate of the spurious signal at this stage was particulate matter trapped in the holes that might have turned from non-conductive to conductive material suddenly when the applied voltage was high. As a standard fix to this suspected reason, the chamber was left at an input of 4kV for 3h in order to burn out any particulate matter that might be trapped inside the GEM foils. A rapid ramp up was performed after this, how ever the problem still persisted but this time started to appear at a lower voltage of 4kV .

At this moment the a diagnostic scan was performed using the oscilloscope. By altering the threshold on the scope, a strange high frequency long tailed signal was observed as opposed to the sharp peaked low frequency characteristic of the standard spurious signal. This strange signal shown below, was never observed to this point, where 36 long detectors and 42 short detectors had been assembled and tested successfully.

To avoid choking up of the assembly line, the decision was taken to flush the chamber with pure CO_2 gas to reduce humidity in the chamber, such that QC tests can continue on successive detectors.

4.2 Chamber GE1/1-X-L-CERN-0038

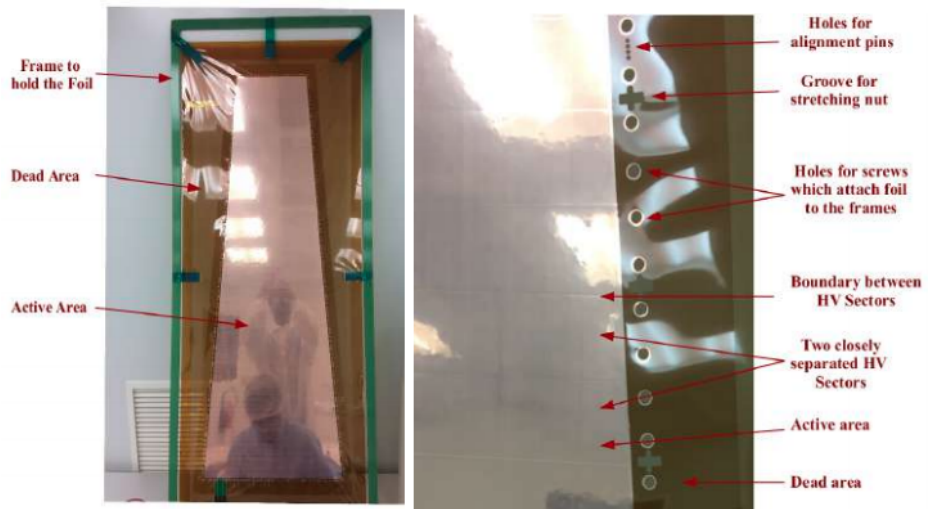


Figure 20: a) Image of one GEM foil still attached to the production frame(left) b) Zoomed in view of the foil attached to the production frame, showing the holes for alignment pins, the screws for the frame, plus-shaped slits for the stretching nuts and the HV Sectors(right)

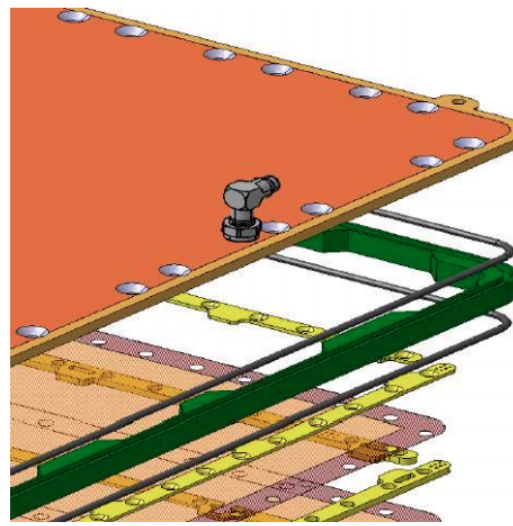


Figure 21: Drawing of the Gas Plug

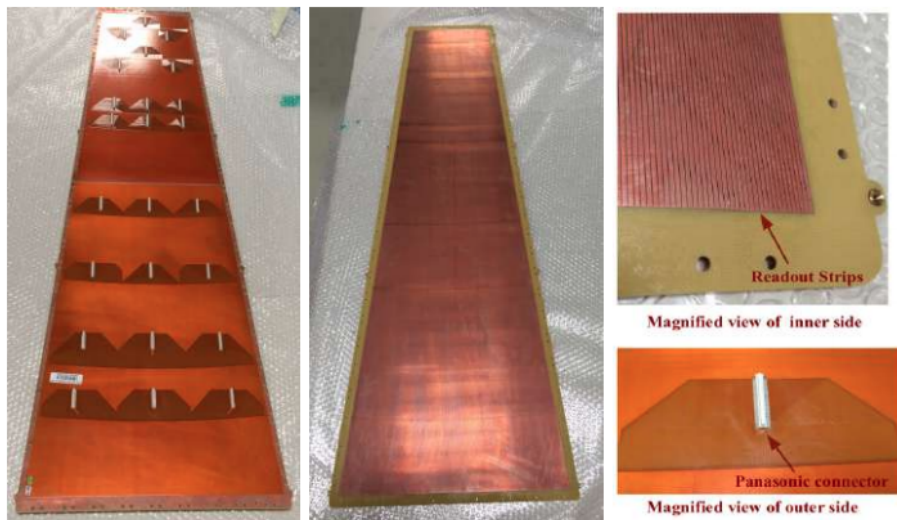


Figure 22: Images of the a) outer side of the readout board b) inner side c) magnified view of the inner side (top) d) magnified view of the outer side (bottom)

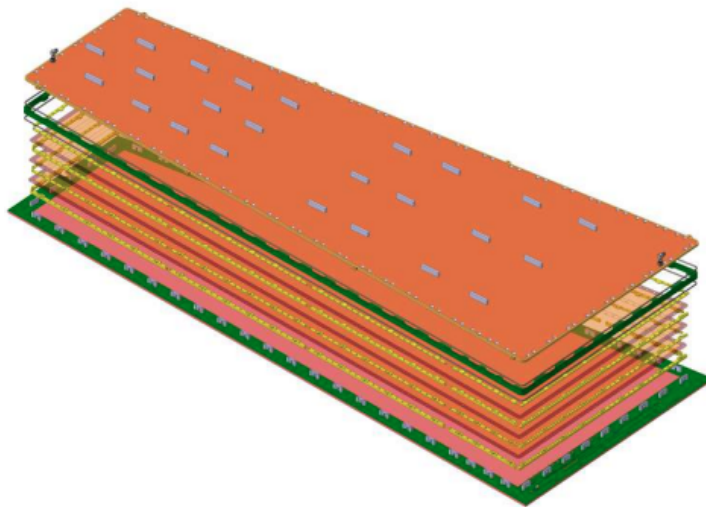


Figure 23: Flow of the assembly procedure

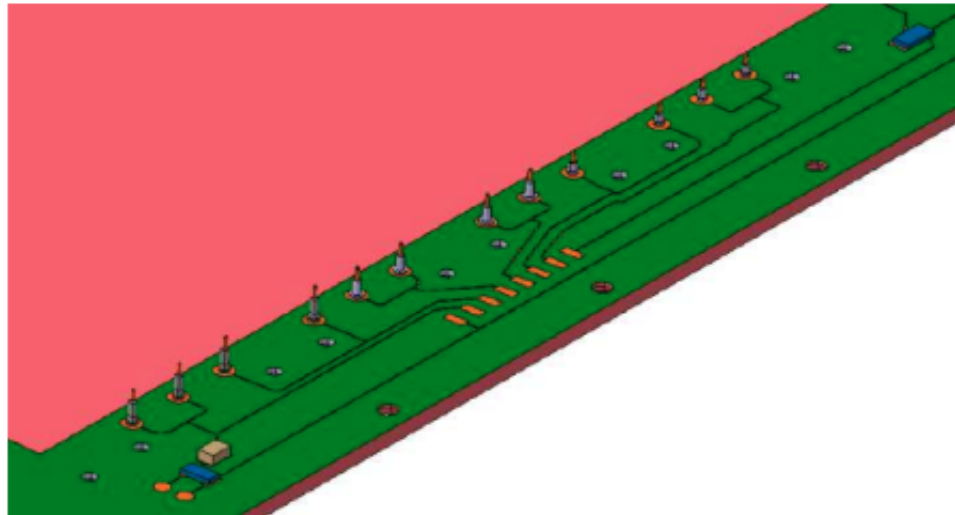


Figure 24: HV circuit arrangement on the drift board

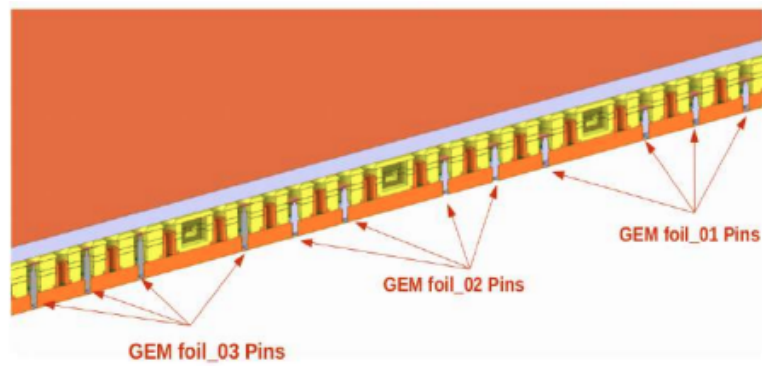


Figure 25: Sliced view showing the spring loaded mechanism of the HV pins and their position on the drift board with respect to the foils

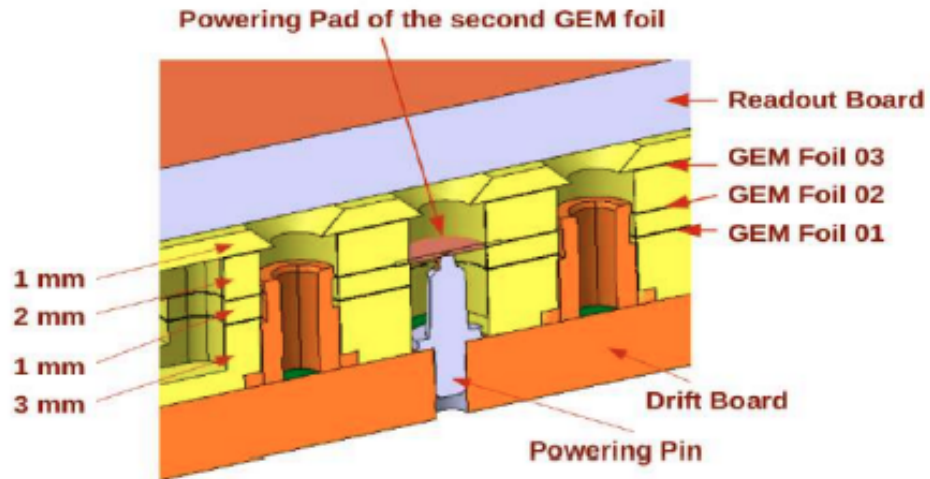


Figure 26: Magnified view of one of the HV pins showing the foil stack and a connection to the GEM Foil 02

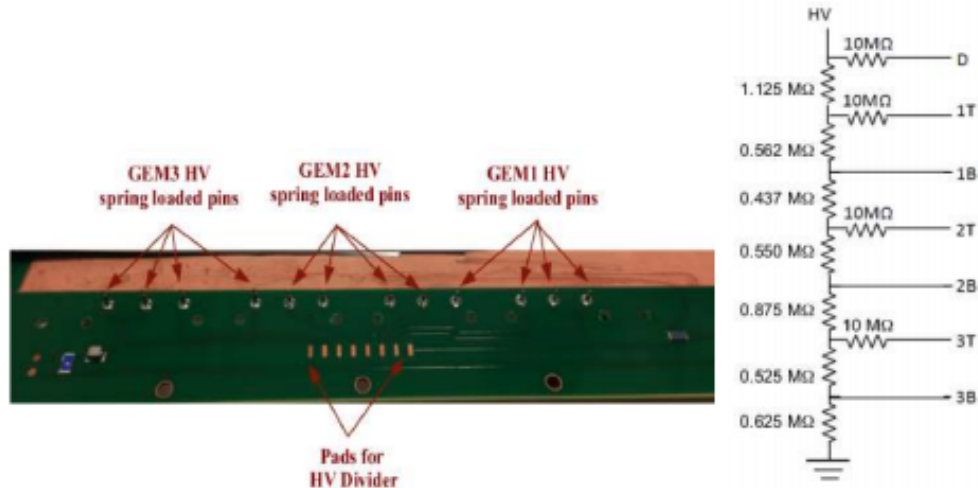


Figure 27: a) Image of the HV circuit arrangement on the drift board (left)
b) Resistive Divider Network used with a single channel power supply (right)



Figure 28: Image of the process of laying the first GEM foil on a Plexiglas base with 3mm internal frames in position

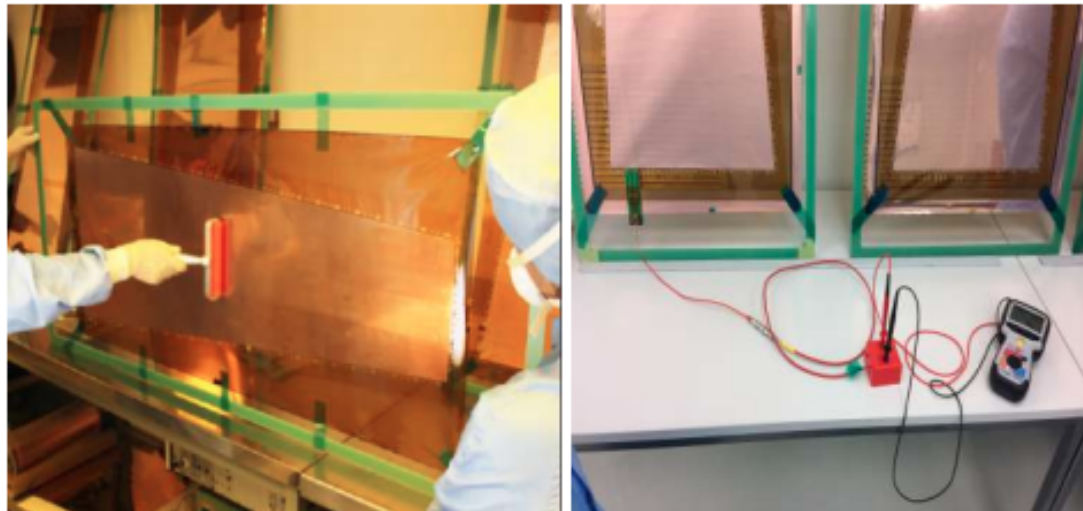


Figure 29: a) GEM foil cleaning using adhesive roller (left) b) Leakage current measurement using MEGGER MIT420 (right)

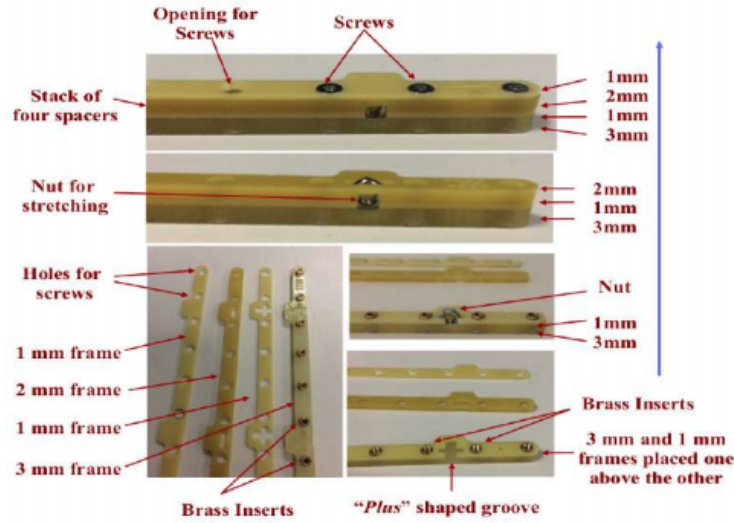


Figure 30: Mechanical structures of the four different internal frames showing the positioning of the brass inserts, grooves for the stretching nuts and positions of fastening screws

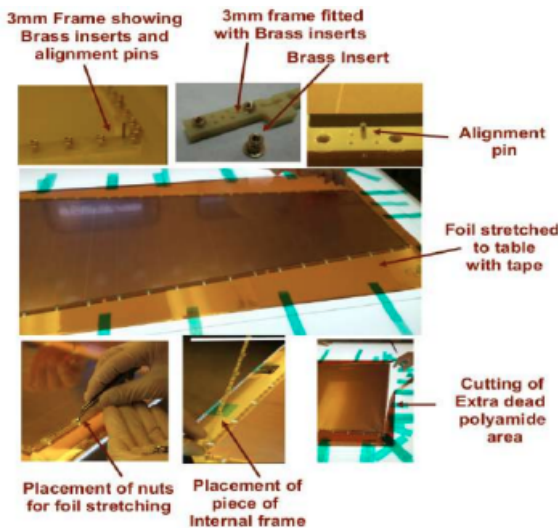


Figure 31: Various steps in the stack formation procedure

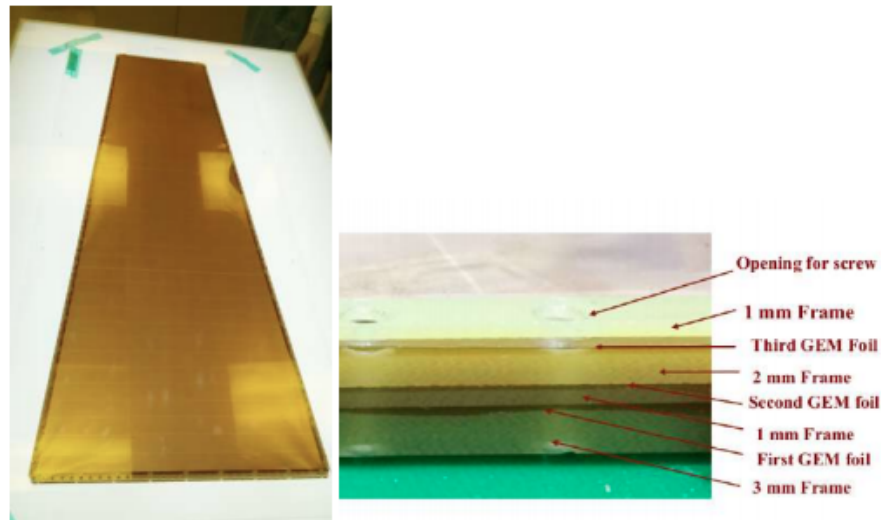


Figure 32: a) The GEM foil stack (left) b) Magnified view of an edge of the stack (right)

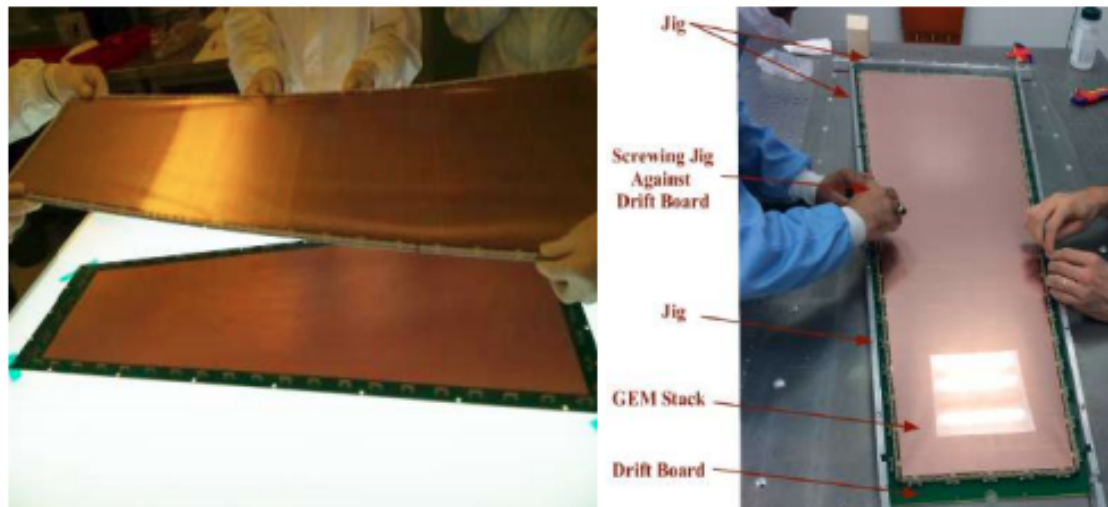


Figure 33: a) Placement of the GEM foil stack on the drift board (left) and (right)

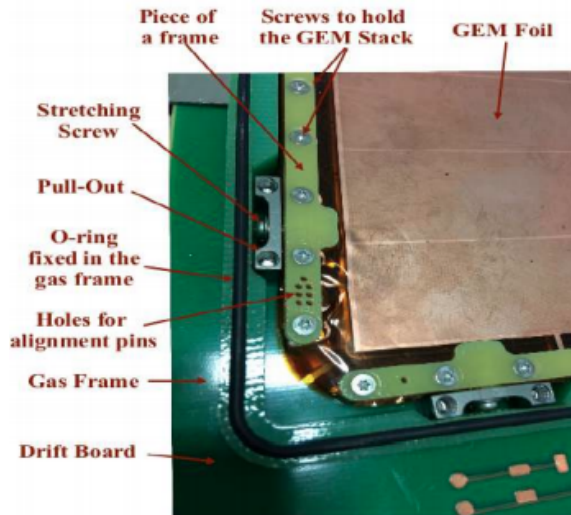


Figure 34: Magnified view of one segment of the chamber before it is closed.



Figure 35: a) Closing of the GEM chamber with the readout board (left) b) The final assembled chamber (right)

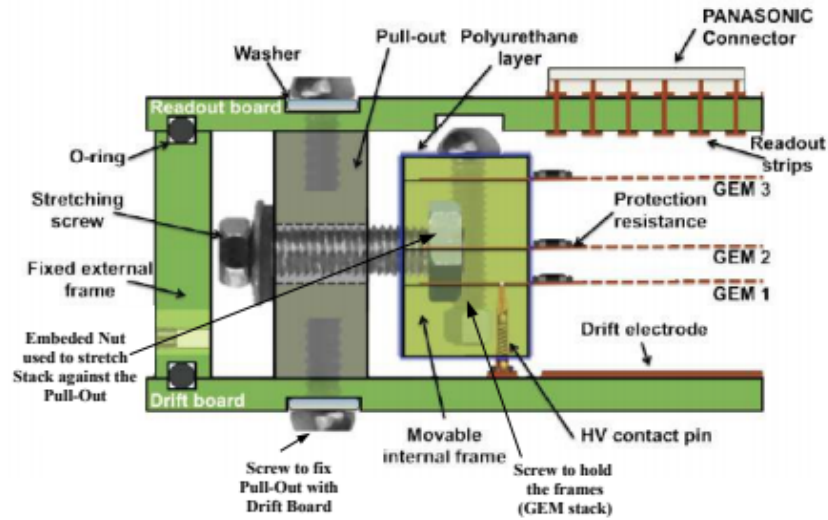


Figure 36: Drawing of the mechanical stretching mechanism

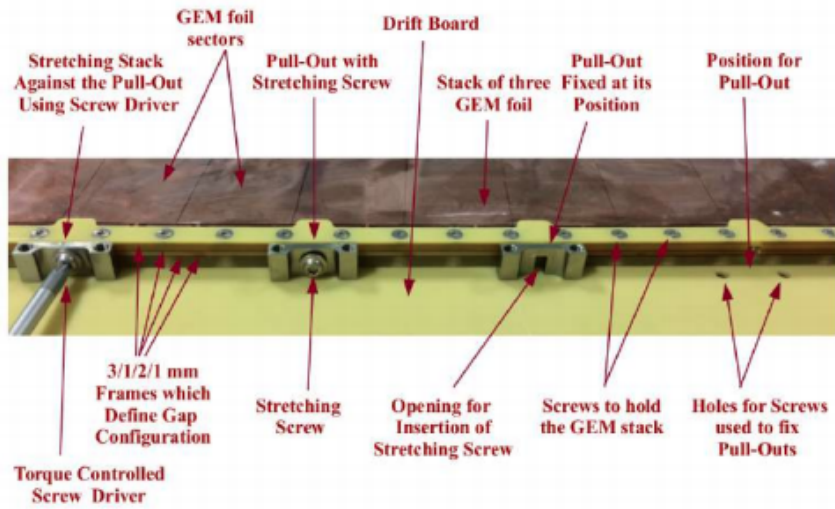


Figure 37: Image of the mechanical stretching mechanism during assembly

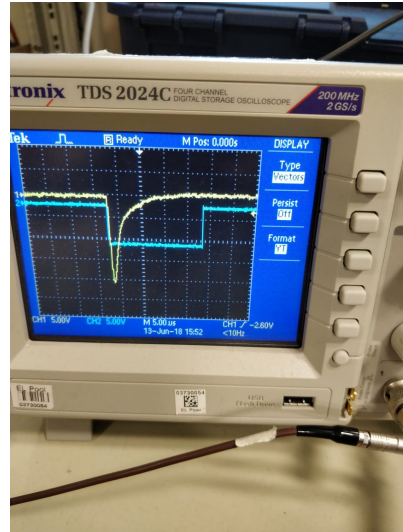


Figure 38: Image of the standard spurious signal in pure CO_2 gas flow

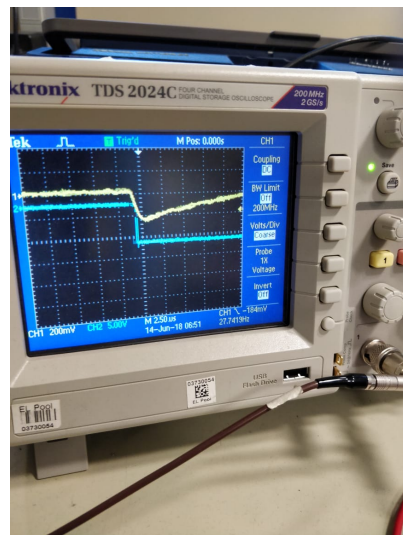


Figure 39: Image of the anomalous long tailed signal

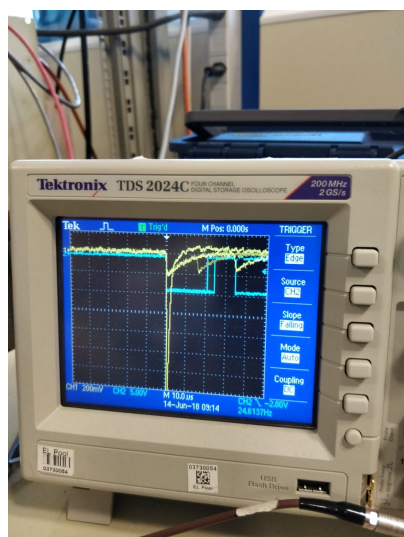


Figure 40: Anomalous long tailed high frequency signal superimposed on a standard spurious signal.